CFD ANALYSIS ON THE SINGLE-PHASE FLOW ELECTRICAL SUBMERSIBLE PUMP PERFORMANCE CURVE

O.M. Kassem[1], A.Q. Abdullah[1], S.S. Dol[1*], M.S. Gadala[1], M.S. Aris[2]

[1]Department of Mechanical Engineering, Abu Dhabi University, Abu Dhabi, United Arab Emirates
[2]Tenaga Nasional Research Sdn. Bhd., Kajang, Malaysia

Email: sharulshambin.dol@adu.ac.ae

ABSTRACT

Most of the industrial fields, especially oil and gas, involve the application of electrical submersible pump (ESP) for flow transport. The pump performance will deteriorate depending on conditions of usage. The main parameters that affect or influence the pump performance curve are pump types, fluid flow rates, gas fractions, the impellers' geometry, rotational speeds and fluid properties. In this work, the pump performance curve was studied as the governing parameters such as flow rates, meshing elements and turbulence models were varied. A computational fluid dynamics simulation (CFD) was applied and the findings were compared with the manufacturer's data for single-phase flows. The main purpose was focused on getting the right technique to investigate this problem. The various turbulence CFD models were analysed and sources of errors were explained. The corresponding pump head losses were discussed and the main improvement or the criteria to obtain the highest efficiency were suggested. The results show that the k-epsilon with enhanced wall treatment is the best CFD technique since it produces the most accurate results and the least errors by allowing flexibility in large pressure gradient and rapid changes in flow properties.

***Keywords**: ESP, CFD simulation, head loss, performance curve, turbulence models*

INTRODUCTION

The electrical submersible pump (ESP) system is a design variation of the centrifugal pump whereby the fluid source is typically located below the discharge datum. It is the second most widely used artificial lift method in the oil and gas industry and the largest (in volume) type of pump produced. In the oil and gas industry, pumps are generally used to boost pressure and to transfer fluids from underground to ground level [1]. However, ESP consists of many parts that are used especially for offshore oil production and it was assembled in a series of stages as shown in Figure 1 that each stage consists of an impeller associated with a diffuser. The impeller connects and rotates with a shaft, which is used to increase the kinetic energy of the flow and then it leaves the diffuser a stationary part used to change the kinetic energy to potential energy and guide the flow to the next stage. ESP is known for being highly efficient in working under multi-phase flow, but the performance curves are significantly degraded under the presence of gas [2].

The production rate and the gas inside the pipes and the viscosity of the oil play a huge role in the ESP performance. If the ESP operates within the two-phase flow, then the performance will decrease, and the surge will cause a vibration in the pump which will lead to a reduction in the service life. The bubble behaviour in the pump is still unpredictable that becomes the main characteristic that affects pump performance [4]. All these problems can be considered as losses. The actual head for ESP can be calculated as,

$$H = H_E - H_{friction} - H_{shock} - H_{leakage} - H_{recirculation} - H_{diffuser} - H_{disk} \quad (1)$$

where is the Euler head, is the head loss due friction, is the head loss due shock, is head loss due leakage, head loss due to recirculation, is head loss inside the diffuser and is head loss due to disk.

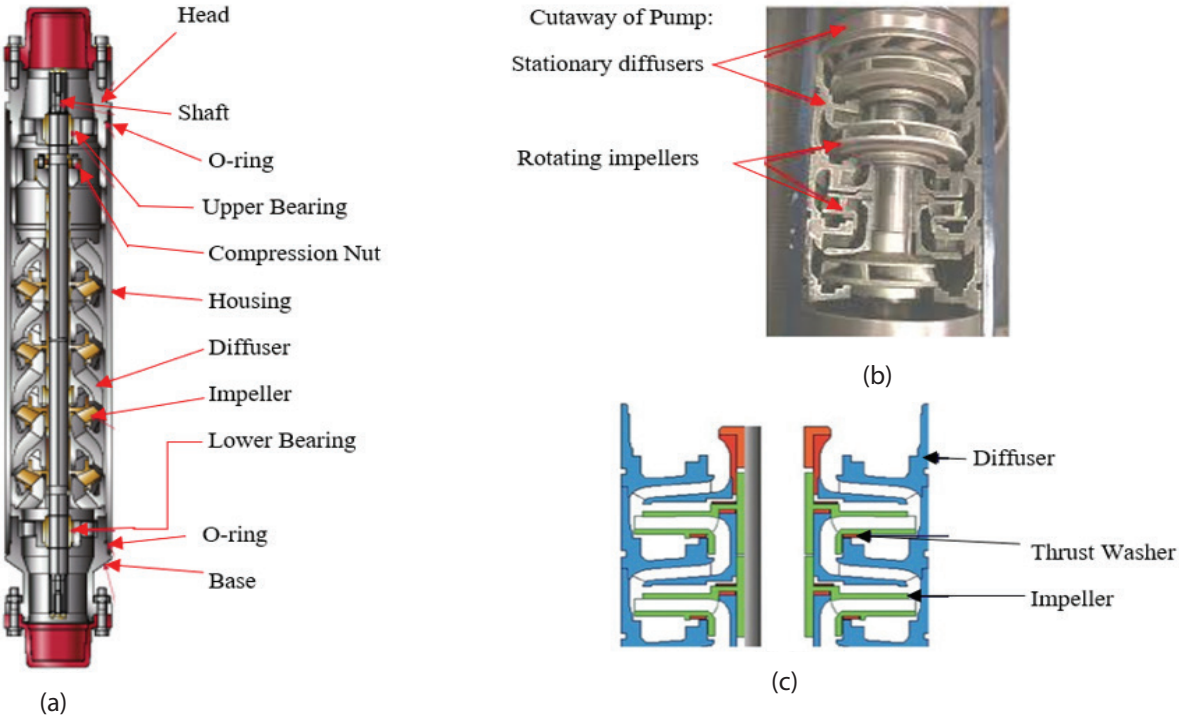

Figure 1 Main parts of single stage ESP (a) multistage pump component (b) cutaway of pump (c) impeller & diffuser [3]

When the pump is rotating, the pumping fluids will cause a difference in velocities between rotating impeller, fluid intake as well as discharge. The velocities occurring in the impeller is the main parameter that can formulate the Euler Head as well as performance curve. Figure 2 represents the velocity triangle at the impeller inlet and outlet.

The Euler pump head, which is shaping the performance curve can be calculated as the following,

$$H_E = \frac{U_2 C_{2U} - U_1 C_{1U}}{g} \tag{2}$$

where U is the impeller tangential velocity, C_U is the fluid tangential velocity at the impeller, and g is the gravity acceleration [5].

The shock loss occurs at the entrance and the exit of the impeller and the shock loss will consider zero at the best efficiency point [BEP]. If the flow rate is different from the designed flow rate, the shock loss will be significant. According to Thin et al. [6], the shock loss occurs because of the mismatching between the flow and the metal angle and it is given by the flowing equation;

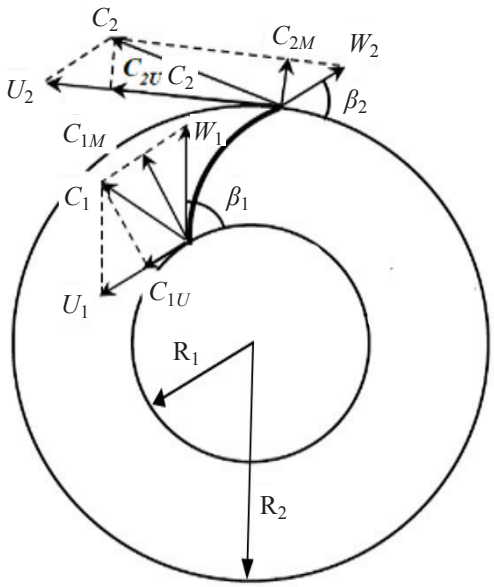

Figure 2 Velocity triangles at impeller inlet and outlet

$$H_{shock} = K(Q - Q_{BEP})^2 \tag{3}$$

where *K* is the empirical constant, and is the flow rate at the best efficiency point.

The frictions losses will play a big role in high flow rates but the leakage loss will be more effective at

low flow rates. The leakage will be decreased by increasing the liquid flow rates and the leakage mainly happened between the stationary parts and the rotating parts. According to the study done by Bing et al [7], the leakage can be obtained by the following equation,

$$H_{leakage} = \frac{Q_{lk} U_{lk} U_2}{2Q^* g} \quad (4)$$

where Q_{lk} is the volume of leaked fluid, U_{lk} is the velocity of the fluid leaked out, and Q^* is ideal flow rate of the pump.

Bing et al. [7] studied the recirculation loss and claim that the recirculation loss happened due to the adverse gradient pressure difference between the inlet and the outlet of the impeller. Moreover, this loss will increase as the liquid flow rate decreases, because if the liquid flow rate decreases then the adverse gradient pressure will increase.

The diffuser loss mainly occurs in the diffuser walls and it is mostly close to the friction loss and the formula was given as the following,

$$H_{diffuser} = \frac{F_\gamma F_\beta f Q^2}{8 g D_H \pi^2 {b_m}^2 \sin^3 \beta_m} \frac{r_{1dif} - r_{2dif}}{r_{1dif} * r_{2dif}} \quad (5)$$

According to Amaral [8] the formula of the diffuser loss mostly related to the difference in pressure and the velocity in the diffuser, as shown in the following equation,

$$H_{diffuser} = \frac{({V_{2d}}^2 - {V_1}^2)}{2g} - C_p \frac{{V_1}^2}{2g} \quad (6)$$

where $C_p = \frac{p_1 - p_2}{0.5 {V_1}^2}$, $V_{2d} = \frac{Q}{\pi (r_{2diff}^2 - r_{1diff}^2)}$ and V_1 is fluid velocity at the inlet. Zhu and Zhang [9] was studying the mechanistic modelling of ESP boosting pressure under gassy flow conditions and they mentioned three types of losses namely, friction, turn, and leakage. The turn losses occur when the flow enters the impeller or gets out from the diffuser due to changes in direction of the flow. The following equation represents the turn losses in the diffuser,

$$H_{diffuser} = f_{TD} \frac{{V_D}^2}{2g} \quad (7)$$

where f_{TD} is the local drag coefficients.

The disk loss is occurring due to contact between the fluid and rotating disk, these contacts make the pump required more power to rotate the disk that delayed by the fluid viscous and shear forces. Some researchers assume the disk losses to be flowing mechanical losses group and others assume it as a separate group, but this model still questioned to deduce the most appropriate prediction. Thin et al. [6] state a model of disk losses, the disk losses is proportional to the power fifth of the disk radius and the friction coefficient () increases with increasing the angle of the developed outlet section of the disk,

$$H_{disk} = \frac{f_{disk} \rho \omega r^2}{10^9 Q} \quad (8)$$

Computational fluid dynamics (CFD) is normally used to model and simulate the ESP problems due to the complexity of the set-up. Therefore, proper CFD approach must be applied depending on the pump operating conditions that are normally operated at the fully turbulence mode. Many improvements have been done on the turbulent models to improve accuracy and computational time. The type of models that should be decided carefully in order to get reasonable results that could be meaningful for industry. Therefore, this paper will focus more on studying the single-phase performance curve behaviour and its effective parameters. Source of errors will be discussed accordingly.

METHODOLOGY

In this paper, the turbulence models of k-omega SST and k-epsilon Standard, Standard with enhanced wall treatments and realizable with enhanced wall treatments are implemented with VOF and Eulerian-Eulerian for single-phase flow by using ANSYS Fluent. The dynamic mesh and the sliding mesh were applied in the interface between the stationary part and the rotary part. The geometry combines the impeller and diffuser of ESP. The number of mesh element used 3, 5, 8 and 13 Million. The turbulence models are applied in the setup option in ANSYS.

Computational Model

Newton's second law state that any change in the momentum in specific volume will be due to the flow of the fluid and the external forces acting in the volume. The conservation of momentum for single-phase that used in ANSYS is given in the following formula,

$$\frac{\partial}{\partial t}(\rho\vec{v}) + \nabla\cdot(\rho\vec{v}\vec{v}) = -\nabla p + \nabla\cdot(\bar{\bar{\tau}}) + \rho\vec{g} + \vec{F} \qquad (9)$$

ρ is the static pressure, $\bar{\bar{\tau}}$ is the stress tensor (described below), and $\rho\vec{g}$ is gravitational body force. $\vec{F}$ is external body force and also contains other model-dependent source terms such as porous-media and nuser-defined sources.

$$\bar{\bar{\tau}} = \mu\left[(\nabla\vec{v} + \nabla\vec{v}^{T}) - \frac{2}{3}\nabla\vec{v}I\right] \qquad (10)$$

where μ is the molecular viscosity, I is the unit tensor, and the second term on the right-hand side is the effect of volume dilation.

Geometry

The type of the pump simulated in this paper will be GDIWA-15T ESP and the geometry will have the combination of casing, impeller, and diffuser, as shown in Figure 3. The geometry will be divided into three Fluid Zones because it is necessary to focus on the critical area, which is called Vaneless area and this area is located between the impeller and the diffuser. The impeller will be specified as a rotary part and the diffuser as a stationary part. The number of blades in the impeller will be 4 blades while 4 outlets in the diffuser. A research was done by Abo Elyamin et al. [10] and they found that the best number of blades is 7. As the number of blades is increased, the friction loss increases due to the increased surface area.

The inlet diameter in the Vaneless area is different than the Outlet diameter as seen in the figure above. In the geometry part, all faces will be selected and be named including the interfaces. After selecting all the faces and dividing the fluid Zone to three parts, the number of the bodies will be 8 (impeller, Diffuser, 4 Fluid Zone in diffuser, Fluid zone 1, Fluid Zone 2). The following Table 1 shows the main dimensions for ESP geometry.

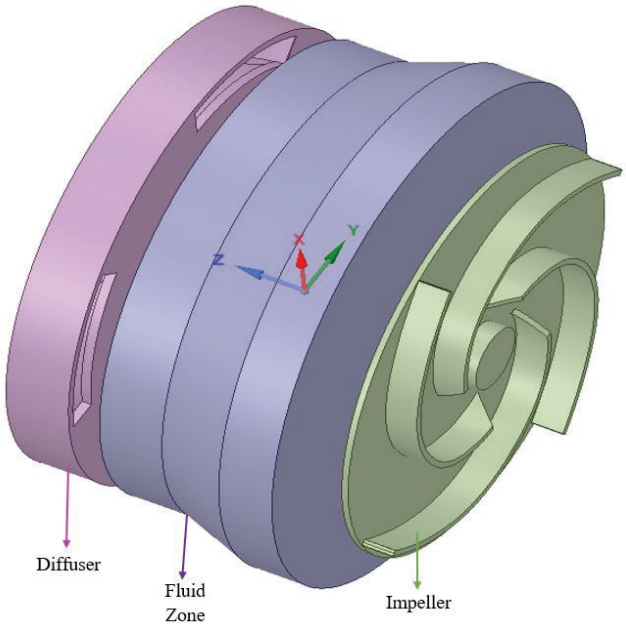

Figure 3 ESP geometry

Table 1 ESP geometry dimensions

Parts	Size
Shaft radius	3.4 mm
Fluid inlet	22.5 mm
Impeller inlet diameter	44 mm
Impeller outlet diameter	144 mm
Blade height	10 mm
Blade thickness	2 mm

Mesh

As the number of elements is increased, the accuracy of the results will also increase, so the number of elements in the impeller and the diffuser will be studied on 3, 5, 8 and 13 million elements and then the proper number of elements will be selected for future work [11]. The element type will be 3D Tetrahedrons and the advantages of this type will be reducing the number of elements to solve the problems that acquire in skewness, increase the convergence rate and give accurate results when complex geometry used [12]. The mesh will be concentrated in main areas by using face sizing. Mostly the gap between the impeller and the diffuser (Vaneless area) is critical so the meshing will be focused more on this area and the type of the mesh is sliding mesh. The following Figure 4 shows the meshing shapes:

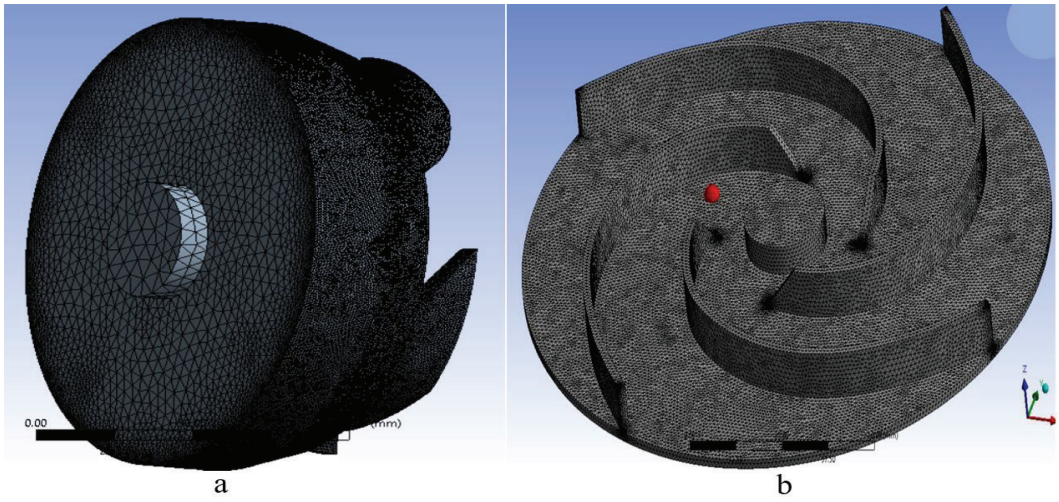

Figure 4 Meshing shapes (a) Final Meshing (b) Impeller mesh

In the meshing part, it is necessary to give names to all the Selection faces to specify the type of each faces later in the setup part.

Setup

In the setup part, the turbulence models chosen in this study are k-omega SST and k-epsilon Standard, Standard with enhanced wall treatments and realizable with enhanced wall treatments [13]. The impeller will be specified as a rotary part with a rotational speed of 2850 rpm in the boundary conditions; while the other parts will be specified as stationary. It is important to specify the interfaces between the fluid zones. The fluid chosen in this study is water and the parameters should be changed to SI units. The number of iterations reaches 500 to get a good result. The flow rate will be from 20 to 420 m^3/s. The inlet face will be changed to velocity inlet and the outlet faces will be as pressure-outlet.

RESULTS AND DISCUSSION

It is important to ensure that the trend of the pump performance curve of the single-phase using CFD is similar to the manufacturer performance curve, so CFD simulation was done in single-phase flow at 10 different flow rates. Figure 5 shows the trend of the curve was almost similar to the manufacturer's curve. As noticed the head decreases when the flow rate increases. Moreover, it is obvious that the error decreased as the flow rate increases and according

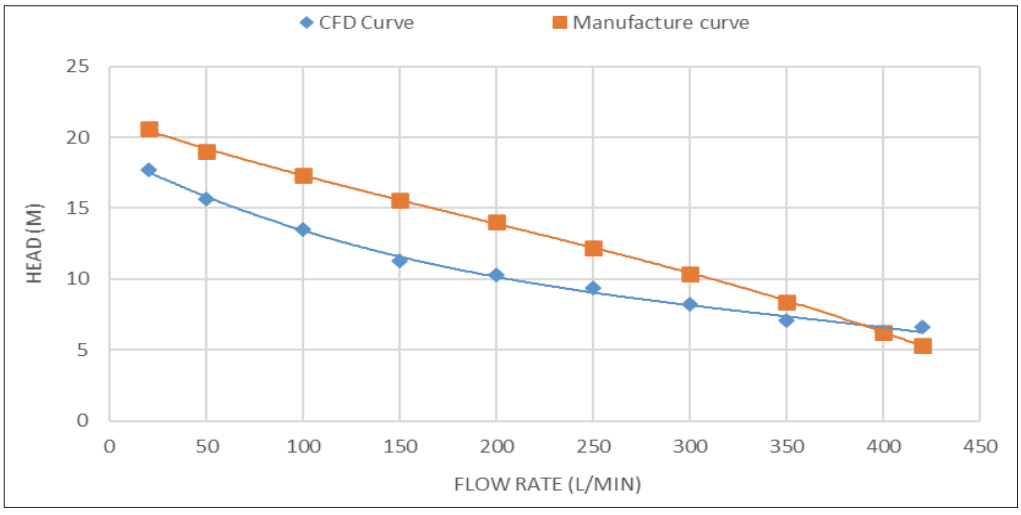

Figure 5 Single-phase performance curve comparison

to [11] the explanation for this deviation, can be attributed to the lack of leakage flow inside ESPs in CFD simulations. The analysis was discussed before in the literature review and it says that as the flow rate decreases the leakage loss increases and therefore decrease the efficiency. Since the leakage flow is not considered at the interfaces, the results will be slightly different from the manufacturer's curve and affinity law predictions.

Mainly the other losses occur in the pump at a high flow rate as mentioned in the literature review but the leakage loss occurs at a low flow rate, and this is the reason for the errors occur at a low flow rate in CFD simulation [14]-[15]. Another source of the error is when the blade curves of the impeller and the diffuser were drawn, the blades were not exactly similar to the actual curve due to the geometry complexity. Similar things were done for the diffuser and because of that, the results would be affected since the angle of the flow at the exit changed thus modifying the flow patterns.

The previous Figure 5 simulation was done at 8 million meshing elements with using k-omega SST model so it is good to see what is the effect of the number of the elements on the accuracy of the results. The following Figure 6 is the performance curve results for various meshing elements.

As seen in Figure 6, as the number of the elements is increased, the accuracy will increase especially in the low flow rates. On the other hand, using 8 million elements on the high flow rate will be the same as using 13 million and that may be saving more computational time.

According to Salehi [4] the k-epsilon standard is giving more error percentages than k-omega but both are close to each other and that was demonstrated in this result in which k-epsilon standard has more error percentage but close to k-omega, as shown in Figure 7. On the other hand, k-epsilon with using enhanced wall treatment is the best choice to be used in single-phase flow [16]-[17]. Both k-epsilon

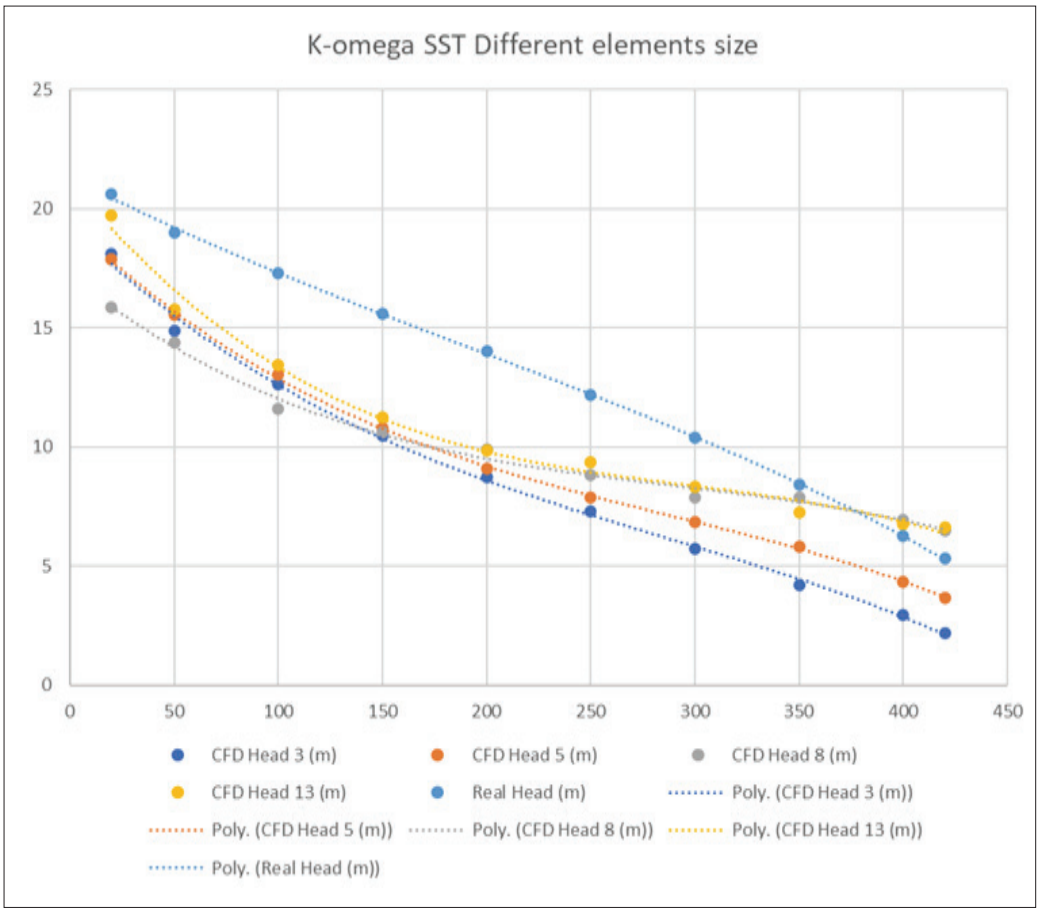

Figure 6 Meshing elements performance comparison

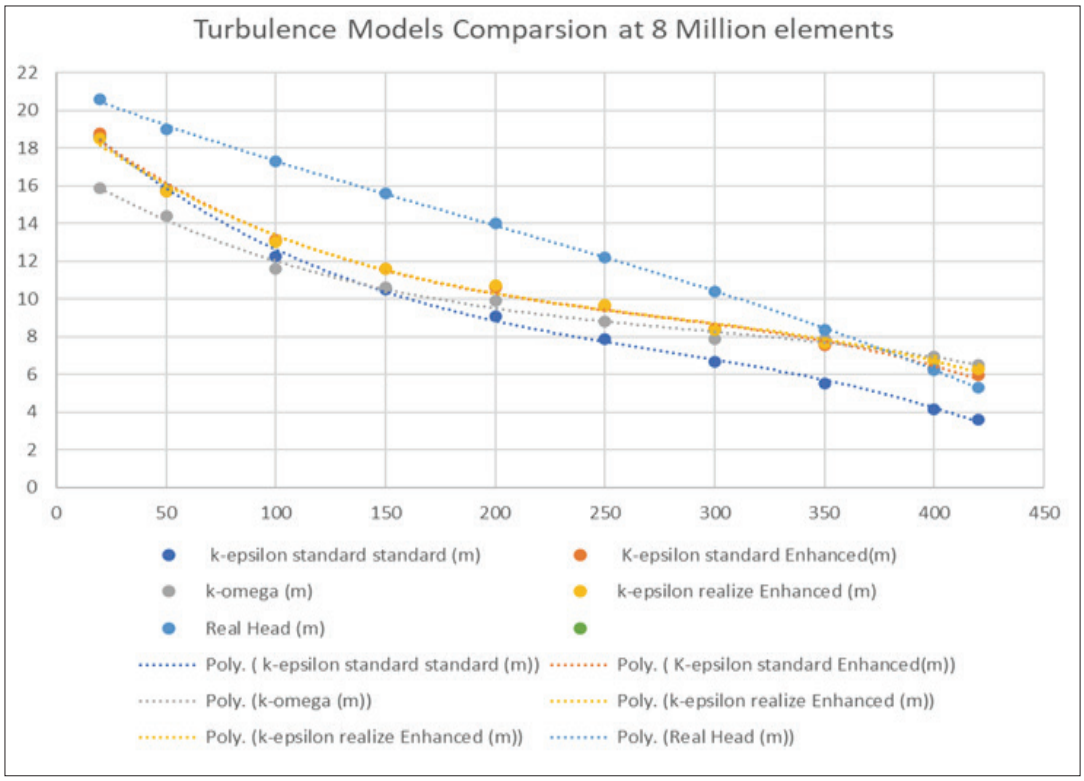

Figure 7 Comparison of the Turbulence models

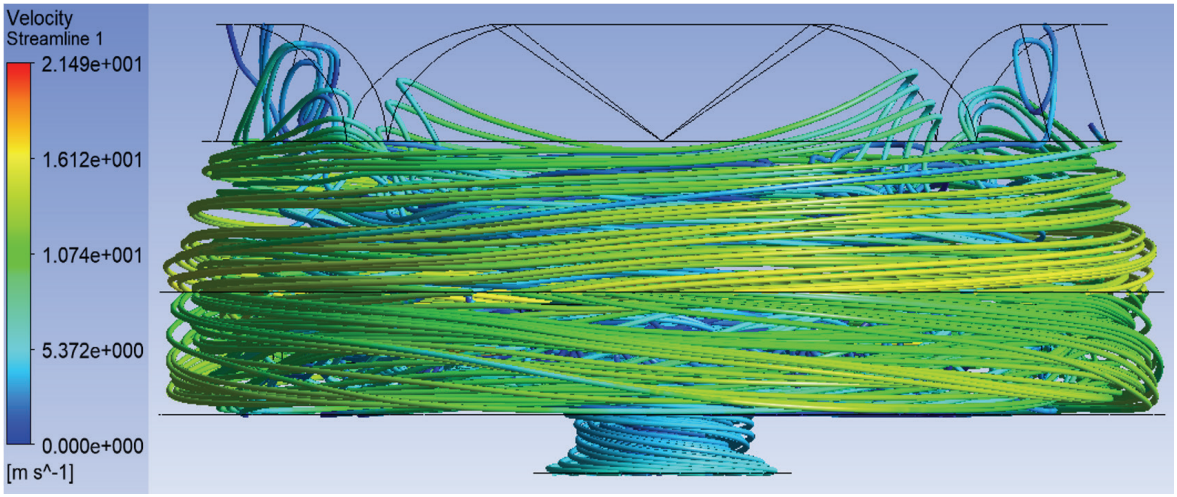

Figure 8 Side view of the velocity streamline

standard enhanced and realizable enhanced are very close to each other as seen in the figure. The reason that the Enhanced Wall treatment is the best choice is because the enhanced wall function allows the fully turbulent law to be easily modified and extended to take into account other effects such as pressure gradients or variable properties, also guarantees the correct asymptotic behaviour for large and small values of and reasonable representation of velocity profiles [18]-[20].

The flow profile is more presented in the form of streamline starts from the inlet until it reaches the outlet. Figures below show the streamline contour at 20 L/min flow rate and 2850 rpm rotation speed,

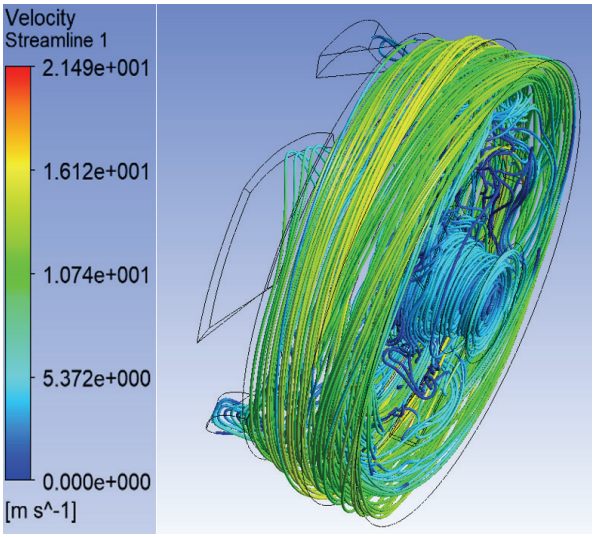

Figure 9 Isometric view of the streamline

The flow path shown in the streamline takes a circular motion due to the forces applied from the impeller rotation. The rotational direction of the impeller is counterclockwise. However, once it leaves the impeller zone, it decelerates the diffuser to change the kinetic energy to potential (pressure). The flow path will be clearer in figure 10. The observed results show that less fluid concentration occurs between the blades due to stall phenomena occurring [21-22].

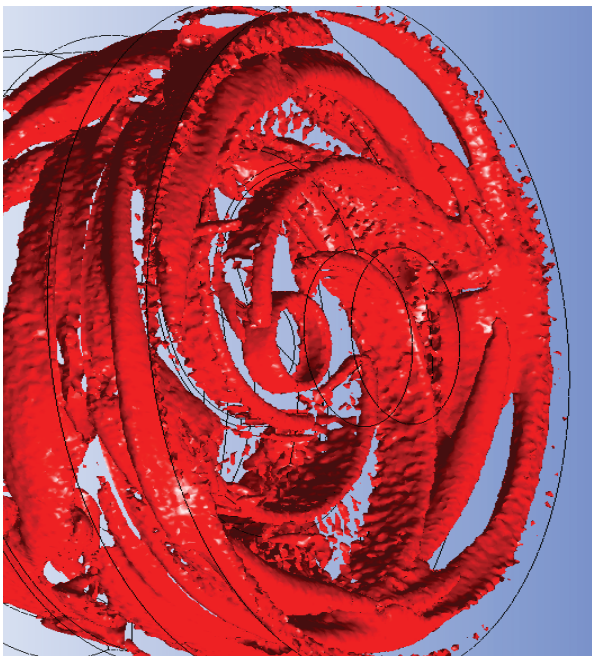

Figure 10 Flow path inside the pump at 20 L/min flow rate

CONCLUSION

CFD simulations of the single-phase flow were conducted to check the suitability of the models in ESP flow problems. The velocity and the pressure inside the impeller and the diffuser were the main parameters analyzed in this study. Different size of mesh elements was studied and compared with the manufacturer's data. The results in this paper can be summarized as the following,

1. CFD is a reliable useful tool for studying and analysing the pump performance.
2. As the mesh elements increase the numerical accuracy increased until it reaches a certain limit then it will remain constant.
3. The number of mesh elements used in this study was 3, 5, 8 and 13 Million elements and the best choice is to use the 13 million elements for single-phase flow.
4. Single-phase simulation results at low flow rates are lower than the manufacturer's data and that due to the leakage flow was not taken in count in the interfaces in the CFD simulation while at high flow rates are almost similar to each other because there will be no leakage in high flow rate in the actual pump.
5. K-epsilon with the Enhanced Wall treatment gives the best result compared with other models because the enhanced wall function allows the fully turbulent law to be easily modified and extended to take into account other effects such as pressure gradients variable properties.

REFERENCES

[1] S.F. Wong, S.S. Dol, S.K. Wee & H.B. Chua, "Miri light crude water-in-oil emulsions characterization: Rheological behaviour, stability and amount of emulsions formed", *J. Pet. Sci. Eng.*, 2018. Doi: 10.1016/j.petrol.2018.02.013.

[2] U. Azimov, E. Tomita, N. Kawahara, &S. S. Dol, "Combustion characteristics of syngas and natural gas in micro-pilot ignited dual-fuel engine", *International Journal of Mechanical and Mechatronics Engineering*, 6, 12, pp. 2863-2870, 2012.

[3] Production Technology, 28 April 2017. [Online]. Available: https://production-technology.org/pump-performance-curves/.

[4] E. Salehi, J. Gamboa & M. Prado, "Experimental studies on the effect of the number of stages on the performance of an electrical submersible pump in two-phase flow conditions", WIT Press, 2013. Doi: 10.2495/FSI130201.

[5] Q. Jiang, Y. Heng, X. Liu, W. Zhang, G. Bois & Q. Si, "A review of design considerations of centrifugal pump capability for handling inlet gas-liquid two-phase flows", *Energies*, 12, 6, 2019. Doi: 10.3390/en12061078.

[6] K.C. Thin, M.M. Khaing & K.M. Aye, "Design and Performance Analysis of Centrifugal Pump", *World Acad. Sci. Eng. Technol.*, 2008.

[7] H. Bing, L. Tan, S. Cao & L. Lu, "Prediction method of impeller performance and analysis of loss mechanism for mixed-flow pump", *Sci. China Technol. Sci.*, 2012. Doi: 10.1007/s11431-012-4867-9.

[8] Amaral, "Single-Phase Flow Modeling of an ESP Operating with Viscous Fluids", Master's Thesis, State University of Campinas, Campinas, São Paulo, Brazil, 2007.

[9] J. Zhu & H. Q. Zhang, "CFD simulation of ESP performance and bubble size estimation under gassy conditions", SPE Annual Technical Conference and Exhibition, 2014. Doi: 10.2118/170727-ms.

[10] G.R.H. Abo Elyamin, M.A. Bassily, K.Y. Khalil & M.S. Gomaa, "Effect of impeller blades number on the performance of a centrifugal pump", *Alexandria Eng. J.*, 58, 1, 2019. Doi: 10.1016/j.aej.2019.02.004.

[11] J. Zhu, H. Zhu, J. Zhang & H.Q. Zhang, "A numerical study on flow patterns inside an electrical submersible pump (ESP) and comparison with visualization experiments", *J. Pet. Sci. Eng.*, 173, pp. 339-350, 2019. Doi: 10.1016/j.petrol.2018.10.038.

[12] H.B. Chan, T.H. Yong, P. Kumar, S.K. Wee & S.S. Dol, "The numerical investigation on the effects of aspect ratio and cross-sectional shape on the wake structure behind a cantilever", *ARPN Journal of Engineering and Applied Sciences*, 11, 16, pp. 9922-9932, 2016.

[13] S.S. Dol & H.B Chan. "Fluid-Structural Interaction Simulation of Vortices behind a Flexible Vortex Generator," *2019 8th International Conference on Modeling Simulation and Applied Optimization (ICMSAO)*, pp. 1-5, IEEE, 2019.

[14] S.S. Dol, H.B. Chan, S.K. Wee & K. Perumal. "The effects of flexible vortex generator on the wake structures for improving turbulence", *IOP Conference Series: Materials Science and Engineering*, 715, 1, p. 012070, 2020.

[15] A. Manivannan, "Computational fluid dynamics analysis of a mixed flow pump impeller," *Int. J. Eng. Sci. Technol.*, 2, 6, pp. 200-206, 2011 Doi:10.4314/ijest.v2i6.63711.

[16] S.S. Dol, H. Chan & S.K. Wee. "FSI simulation of a flexible vortex generator and the effects of vortices to the heat transfer process", *Platform: A Journal of Engineering,* 4, 2, pp. 58-69, 2020.

[17] C. Maitelli, V. Bezerra &W. da Mata, "Simulation of flow in a centrifugal pump of ESP Systems Using Computational Fluid Dynamics", *Brazilian J. Pet. Gas*, 2010.

[18] S.S. Dol, L.V. Fui & A. Ulugbek. "Hybrid RANS-LES Simulation of In-Cylinder Air Flow for Different Engine Speeds at Fixed Intake Flow Pressure", *International Journal of Mechanical, Aerospace, Industrial and Mechatronics Engineering*, 8, 7, pp. 1330-1333, 2014.

[19] M.M. Salek, S.S. Dol & R.J. Martinuzzi. "Analysis of Pulsatile Flow in a Separated Flow Region", Proceedings of the ASME 2009 Fluids Engineering Division Summer Meeting. Volume 1, pp. 1429-438, ASME, 2009.

[20] S.S. Dol, S.K. Wee, H.B. Chan & P. Kumar, "Turbulence Characteristics behind a Flexible Vortex Generator", *Wseas transactions on fluid mechanics*, 14, pp. 1-7, 2019.

[21] M.N.H. Mat, & N. Asmuin, "Optimizing nozzle geometry of dry ice blasting using CFD for the reduction of noise emission", *International Journal of Integrated Engineering*, 10, 5, 2018.

[22] M.N.H. Mat, N.Z. Asmuin, M.F.M. Basir, M. Goodarzi, M.F. Abd Rahman, R. Khairulfuaad & M.S.M. Kasihmuddin, "Influence of divergent length on the gas-particle flow in dual hose dry ice blasting nozzle geometry,", *Powder Technology*, 364, pp. 152-158, 2020.